02

Dielectric Measurements of Nanocrystalline VO_2 : Fe Films

© A.V. Ilinskiy[1], R.A. Castro[2], V.A. Klimov[1], A.A. Kononov[2], E.B. Shadrin[1,¶]

[1] Ioffe Institute of RAS,
194021 St. Petersburg, Russia [2] Herzen State Pedagogical University of Russia,
191186 St. Petersburg, Russia

¶ e-mail: shadr.solid@mail.ioffe.ru

Received July 6, 2022
Revised July 20, 2022
Accepted July 20, 2022

Dielectric spectroscopy methods revealed the existence of two types of relaxation processes in the semiconductor phase of VO_2 : Fe films. The characteristic relaxation times are denoted by τ_1 and τ_2. It is shown that the temperature dependences of τ_1 and τ_2 have hysteresis, the position of the loops of which coincides with the points of the semiconductor-metal phase transition. in VO_2 : Fe films. τ_1 corresponds to undoped, and τ_2 corresponds to Fe-doped nanocrystallites of the VO_2 film. It is shown that the physical mechanism of the relaxation process is due to the establishment of equilibrium after the action of an electric field on conduction electrons. The numerical values of the parameters of the distribution of relaxers over relaxation times are determined.

Keywords: dielectric measurements, correlation effects, vanadium dioxide, VO2, insulator-metal phase transition

DOI: 10.21883/EOS.2022.10.54859.3902-22

Introduction

Dielectric measurements, or otherwise dielectric spectroscopy, according to the definition, is a measurement of the frequency dependence of the permittivity of a material $\varepsilon^* = \varepsilon' + i\varepsilon''$ and related variables in the low and ultra-low frequencies, in particular the dielectric loss tangent, $\mathrm{tg}\,\delta(f) = \varepsilon''/\varepsilon'$ [1]. In the process of dielectric measurements, the parameters of the electrical response of the material to the action of an applied electrical voltage of various frequencies f are determined. During measurements, voltage is applied, as a rule, to the cell in form of a flat capacitor, between the metal plates of which the material under study is placed. Typical permittivity spectra (PS) are the frequency dependences of the complex permittivity of the material $\varepsilon^*(f)$ and its complex impedance $z^*(f)$.

In this work, we will focus on the consideration of the PS of crystalline films of vanadium dioxide ,(and namely, strongly correlated material with a thermal phase transition (PT) semiconductor−metal at $T_c = 67^\circ$C. Thus, in this work,a particular case of dielectric measurements of the parameters of a specific oxide material is considered. The advisability for using the proposed study approach is due to the fact that at present dielectric spectroscopy is rapidly developing in connection with the development and creation of industrial samples of highly sensitive dielectric spectrometers equipped with high-speed computers with modern software.

The purpose of this work was to study the features of the electrical response of a set of nanocrystalline vanadium dioxide grains synthesized on an insulating substrate, which form a thin film. In this case, the PS of undoped films VO_2 and films doped with iron ions, VO_2 : Fe were studied. Such characteristics of the electrical response of the films as the frequency dependences of the complex permittivity $\varepsilon^*(f)$ and their Cole−Cole-diagrams (CC- diagrams). The measurement results are presented by modern dielectric spectrometers both in the form of numerical arrays and in graphical form. In this case, in addition, the possibility of determining the parameters of the Havriliak−Negami relaxation function (function HN), which characterizes the temporal characteristics of the electrical response of the system, is realized.

Experiment procedure

The samples on which the dielectric measurements were performed were thin (100 nm) films of vanadium dioxide (VO_2) synthesized by laser ablation [2] on insulating mica substrates with a thickness of 300 μm. The films were doped with iron ions in the process of synthesis: (VO_2 : Fe). The film morphology was controlled using an atomic force microscope, which made it possible to obtain both images of the film surface with a resolution of 10 nm, both and histograms of the distribution of nanocrystalline film grains by their size. In this work, the PS of such VO_2 films for which the histogram of the size distribution of nanocrystalline grains has one maximum and which in this respect can be called „as the homogeneous ones “, are presented and analyzed,.

Experimental results

In Fig. 1, the results of dielectric measurements of the frequency dependences of the dielectric loss tangent $\mathrm{tg}\,\delta(f)$ of an undoped VO_2 (a) film and a film doped

with iron VO_2:Fe (b) obtained for $T = 20°C$, are shown. Comparison of the spectra shows that when doping with iron in the high-frequency region (10^4 Hz), an additional maximum 2 appears on the PS, which we associate with the appearance in the total mass of grains of an aggregate of nanocrystalline grains subjected to doping.

The PS of a thin iron-doped vanadium dioxide film are presented in more detail in Fig. 2. Here the frequency dependences of the real $\varepsilon'(f)$ and imaginary $\varepsilon''(f)$ parts of the permittivity are shown. These results were obtained by changing the temperature in the range 20−100°C. Fig. 2, *c* shows CC-diagrams obtained on the basis of the data shown in Fig. 2, *a, b* CC-diagram $\varepsilon''(\varepsilon')$ is the dependence of the imaginary part of the permittivity ε'' on its real part ε', and the calculation formula for it can be obtained by eliminating the frequency f as a parameter from the calculation formulas for ε' and ε''. Let's pay attention to the fact that the express analysis of PS presented in the form of CC-diagrams turns out to be more illustrative, since it allows, according to the form of the diagram, to make a qualitative evaluating of dependence of the physical parameters for the sample on characteristics of external conditions by evaluating „of the correctness" for shape of the principal semicircle and its satellites (see details below).

The spectra of the real parts of the permittivity $\varepsilon'(f)$ contain two „steps", and the spectra of the imaginary part $\varepsilon'(f)$ contain two maxima (*1* and *2*). These features of the PS shift towards higher frequencies with increasing temperature. The temperature dependence of the frequency position of the $\varepsilon''(f_1)$ largest maximum demonstrates thermal hysteresis, the loop of which 10°C wide is located at $T_c = 67°C$ (Fig. 3).

The hysteresis loop of the second (smaller) maximum located in the higher frequency region of the spectrum (f_2) can only be partially measured. The fact is that when heated already at temperatures lower than the temperature $T_c = 67°C$, the semiconductor−metal PT in VO_2, namely for $T \sim 60°C$, the high-frequency maximum *2* of the function $\varepsilon''(f_2)$ „goes" sharply to the high-frequency region ($f_2 > 10^7$ Hz), so that the measurement of the hysteresis loop becomes difficult. Nevertheless, it is possible to establish that this loop is located at lower temperatures than the loop of a higher maximum *1*. That is, the hysteresis loop of the maximum *1* is located at $T_c = 62°C$ (the phase transition temperature T_c was taken as the location temperature maximum of the temperature derivative of the branch of hysteresis loop corresponding to sample heating). Note that the presence itself of temperature hysteresis loops indicates that the crystalline grains of the VO_2 film in the region $T_c \sim 60-70°C$ undergo a phase transformation. For VO_2 it is a semiconductor−metal PT [3]. The CC-diagram of the VO_2:Fe film, like the PS, acquires an additional feature after doping and already contains two semicircles, the shape of which, as it turned out, is weakly depends on the temperature in the region $T \leq T_c$.

Turning to the analysis of the experimental results presented in Figs 1−3, one note that such an analysis can be carried out both on the basis of the Debye relaxation theory and on the basis of calculating the electrical impedance of the corresponding equivalent circuits [4]. Here we will focus on the first version of the analysis.

Basics for calculation

The Debye relaxation theory [1] assumes that in the case when the material under study contains one type of relaxation oscillators with a characteristic unique relaxation time τ_1, the frequency dependence of the complex permittivity has the form

$$\varepsilon^*(\omega) = \varepsilon_\infty + \frac{\Delta\varepsilon}{1 + (i\omega\tau_1)}, \qquad (1)$$

where ε_∞ is the high-frequency limit of the frequency dependence function of the real part of the permittivity ε^*, $\Delta\varepsilon$ is the dielectric increment (difference between the low-frequency ε_s and high-frequency ε_∞ limits of the real parts of the permittivity), $\omega = 2\pi f$.

Within this approximation, the frequency spectrum $\varepsilon'(f)$ has one „step", and the spectrum of the dielectric loss function $\varepsilon''(f)$ has one maximum at the characteristic frequency f_1 close to the location „of the step". CC-diagram $\varepsilon''(\varepsilon')$ in this case is a regular semicircle, the center of which is located on the abscissa-axis. Note that the exclusion of the frequency ω in the CC-diagram as a parameter simultaneously leads to the exclusion of the relaxation time τ_1. This leads to independence of the shape of the semicircle from the numerical value τ_1.

If there are several types of relaxation oscillators in the material under study, for example, two types with a single relaxation time τ_1 and τ_2 for each type, then the formula (1) takes the form

$$\varepsilon^*(\omega) = \varepsilon_\infty + \frac{\Delta\varepsilon_1}{1 + (i\omega\tau_1)} + \frac{\Delta\varepsilon_2}{1 + (i\omega\tau_2)}. \qquad (2)$$

In this case $\varepsilon'(f)$ has two „steps", the loss frequency function $\varepsilon''(f)$ i.e. two maxima at frequencies f_1 and f_2, CC-diagram $\varepsilon''(\varepsilon')$ is two regular semicircles of different diameters (the heights of the semicircles at their maxima are equal to half the diameters of the semicircles) (see dotted curves in Fig. 2, calculated by formula (2)). If the times τ_1 and τ_2 differ greatly in their numerical values, then the shape of the semicircles also does not depend on the numerical values of τ_1 and τ_2, but if $\tau_1 \approx \tau_2$, then the semicircles partially overlap (Fig. 2, *c*), and for $\tau_1 = \tau_2$ merge into one regular semicircle.

However, the experimental spectra, as a rule, are more complex than the calculated ones. In our case, the calculated $\varepsilon'(f)$ curves have „steeper" steps compared to the experimental curves, the calculated $\varepsilon''(f)$ maxima turn out to be narrower, and the curve calculated by the formula (2) CC-diagram, having the form of a regular semicircle, differs somewhat in shape from the experimental CC-diagram. Namely, the heights of the semicircles of the

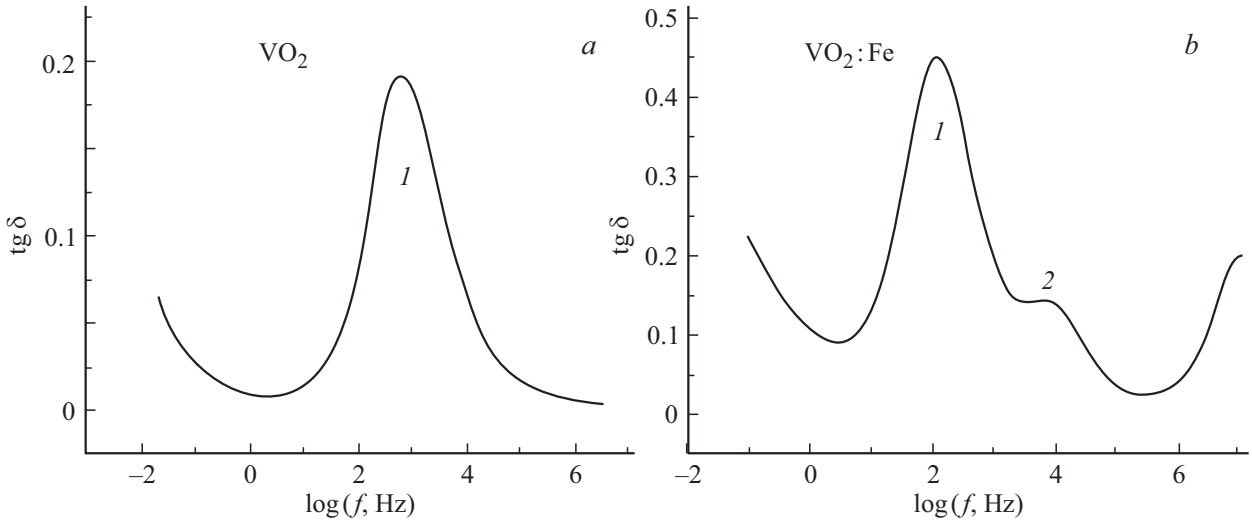

Figure 1. Frequency dependences of the dielectric loss tangent $\mathrm{tg}\,\delta(f)$ of an undoped film VO_2 (a) and a film doped with iron VO_2:Fe (b) obtained for $T = 20^\circ$C.

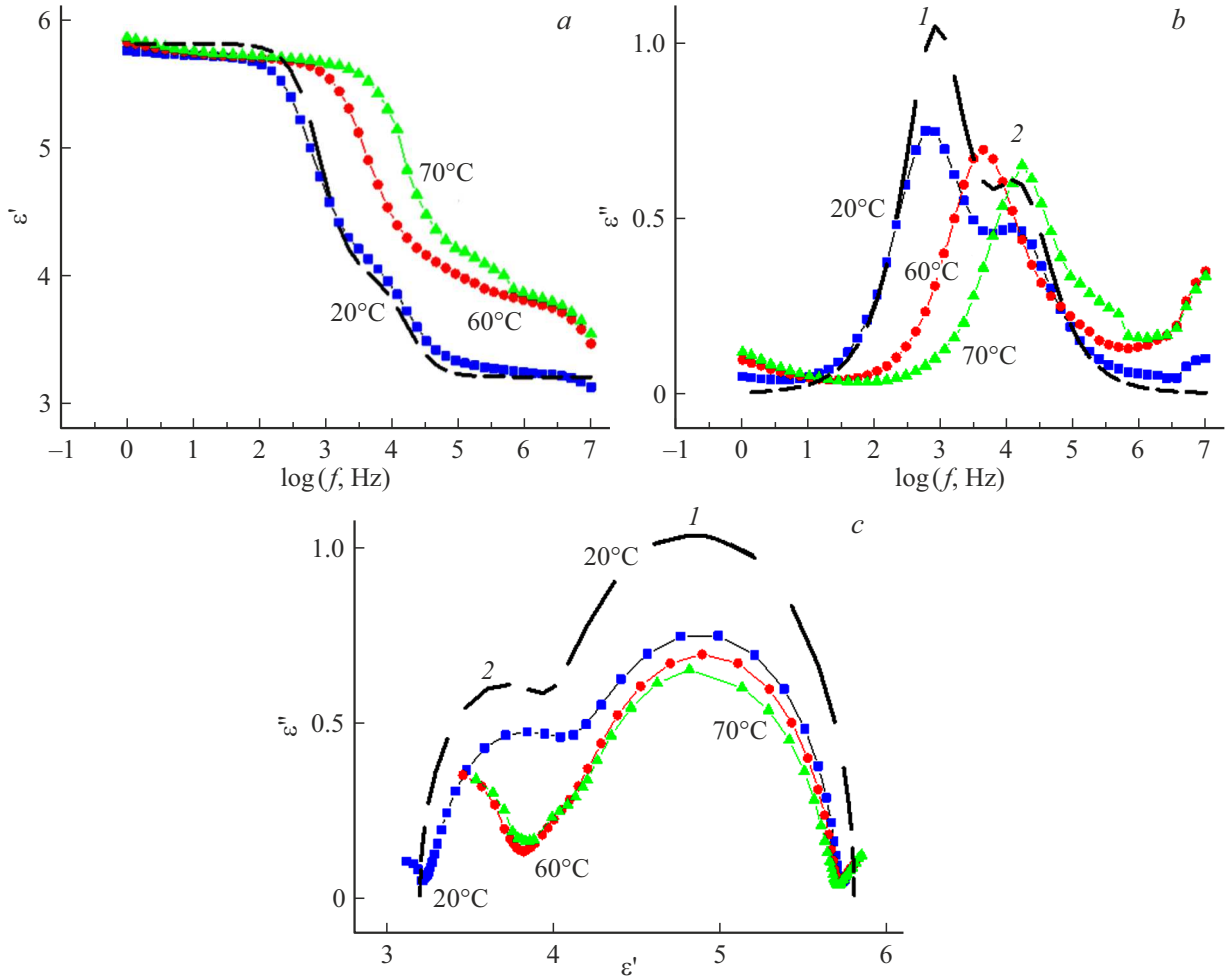

Figure 2. Frequency dependences of the real ε' (a) and imaginary ε'' (b) parts of the permittivity and CC-diagrams (c) for the VO_2:Fe film at various temperatures. Points are from experiment, dotted curves are from result of calculation by formula (2) for $T = 20^\circ$C. *1* and *2* are numbers of maxima.

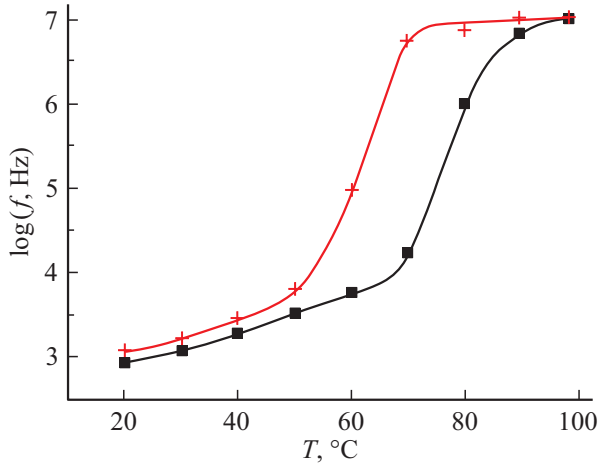

Figure 3. Temperature hysteresis loop of the frequency position f_1 of the maximum *1* (see Fig. 2) of the imaginary part $\varepsilon''(f)$ for the permittivity.

experimental CC-diagrams turn out to be less than half of their diameters. The point is that a real sample can contain several types of relaxation oscillators, and each type can contain a set of individual relaxators with close relaxation times, but with a certain distribution of their temporal density over the numerical values of the times. Different types of relaxation oscillators will appear in this case as several $\varepsilon''(f)$ maxima and semicircles on the CC-diagram. In addition, the presence of a set of individual relaxation oscillators with close relaxation times for each type of relaxation oscillators will manifest itself in the distortion of the shape of the $\varepsilon''(f)$ curves and the shape of the semicircles on the CC-diagram. To take into account these distortions, formula (1) is modernized, transforming to the form [5,6]

$$\varepsilon^*(\omega) = \varepsilon_\infty + \frac{\Delta\varepsilon}{[1 + (i\omega\tau_1)^{1-\alpha}]^\beta}, \tag{3}$$

where α and β are coefficients lying in the intervals $0 \le \alpha < 1$, $0 < \beta \le 1$.

From (3), calculating the power of a complex number, we obtain after extracting the main branch of the multivalued logarithm

$$\varepsilon' = \varepsilon_\infty + (\varepsilon_s - \varepsilon_\infty) r^{-\beta/2} \cos\beta\theta,$$

$$\varepsilon'' = (\varepsilon_s - \varepsilon_\infty) r^{-\beta/2} \sin\beta\theta,$$

$$r = \left[1 + (\omega\tau_1)^{1-\alpha} \sin\left(\frac{\alpha\pi}{2}\right)\right]^2 + \left[(\omega\tau_1)^{1-\alpha} \cos\left(\frac{\alpha\pi}{2}\right)\right]^2,$$

$$\Theta = \operatorname{arctg}\left[\frac{(\omega\tau_1)^{1-\alpha} \cos\left(\frac{\alpha\pi}{2}\right)}{1 + (\omega\tau_1)^{1-\alpha} \sin\left(\frac{\alpha\pi}{2}\right)}\right].$$

As an example, Fig. 4 shows the PS calculated by formula (3) for some values of α and β. At $\alpha \neq 0$ and $\beta \neq 1$ „the steps“ $\varepsilon'(f)$ become slopinger, the functions $\varepsilon''(f)$ in the region of maxima broaden and acquire asymmetry. The indicated changes in the PS are most clearly manifested in the CC-diagrams: at $\alpha \neq 0$ the centers of the semicircles shift down along the ε'' scale, and at $\beta \neq 1$ their shape is distorted

The variables α and β can be determined by analyzing CC-diagrams [5,6] by selecting the values of the coefficients α and β, which make it possible to best match the curves calculated by formula (3) with the results of measurements of the PS. By the obtained values α and β one can judge the degree „of smearing“ of the time distribution of relaxation oscillators and the asymmetry about its maximum of the time distribution within the given type of relaxation oscillators.

From what has been said, it follows that for our case of two types of relaxation oscillators, one should use a more complicated formula than (3) (4)

$$\varepsilon^*(\omega) = \varepsilon_\infty + \frac{\Delta\varepsilon_1}{[1 + (i\omega\tau_1)^{1-\alpha_1}]^{\beta_1}} + \frac{\Delta\varepsilon_2}{[1 + (i\omega\tau_2)^{1-\alpha_2}]^{\beta_2}}. \tag{4}$$

It is possible to achieve good agreement between the calculation results using formula (4) and the measurement results (Fig. 2) by setting the following values of the coefficients: $\alpha_1 = \alpha_2 = 0.1$ and $\beta_1 = \beta_2 = 0.95$. This means that the relaxation oscillators for both sets of grains are distributed over time almost symmetrically and in a rather narrow time region.

The disadvantage of the above consideration by formula (4) is the absence of a specific analytical and graphical form of the distribution of the number of relaxation oscillators over their relaxation times. In order to eliminate this shortcoming, a special method [5,6] was developed to take into account the differences between the experimentally measured PS and the type of spectra given by the Debye relaxation theory. For this purpose, in accordance with the expression

$$\varepsilon^*(\omega) = \varepsilon_\infty + (\varepsilon_s - \varepsilon_\infty) \int_0^\infty \frac{G(\tau)}{1 + i\omega\tau}\, d\tau \tag{5}$$

the distribution function $G(\tau)$ of the temporal density of relaxation oscillators with respect to the relaxation times is introduced into consideration. As such a function that refines the Debye theory, one can use in calculations, for example, the Havriliak–Negami (function HN) [6]. This function contains three variable parameters (τ_{HN}, α_{HN} and β_{HN}) and has the form

$$G(\tau) = \frac{1}{\pi} \times \frac{(\tau/\tau_{\mathrm{HN}})^{\beta(1-\alpha)} \sin(\beta\varphi)}{\left[(\tau/\tau_{\mathrm{HN}})^{2(1-\alpha)} + 2(\tau/\tau_{\mathrm{HN}})^{(1-\alpha)} \cos(\pi[1-\alpha]) + 1\right]^{\beta/2}}, \tag{6}$$

where

$$\varphi = \operatorname{arctg}\left[\frac{\sin(\pi[1-\alpha])}{(\tau/\tau_{\mathrm{HN}}) + \cos(\pi[1-\alpha])}\right].$$

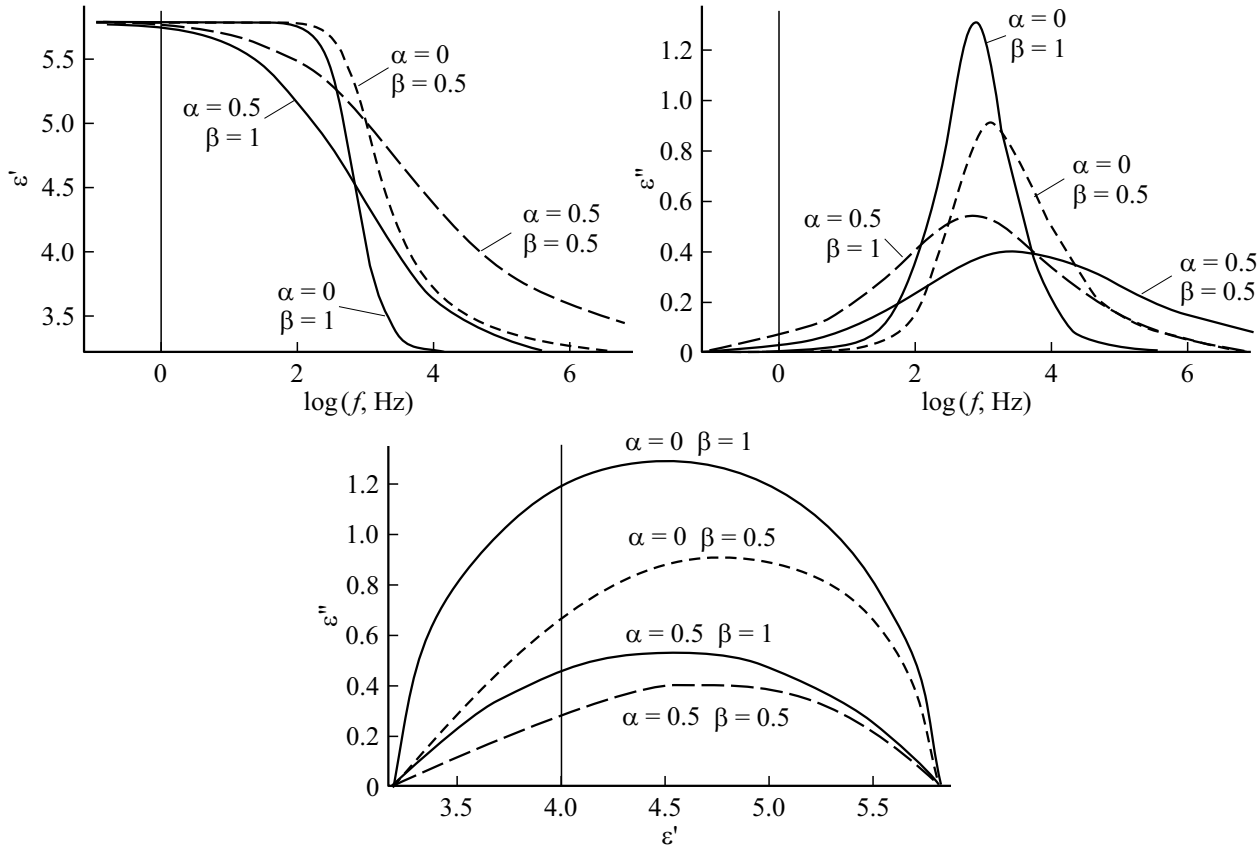

Figure 4. PS (ε' and ε'') and CC-diagrams calculated by formula (3) for different values α and β.

The parameters of the HN function show the average position of the relaxators on the time scale (τ_{HN}), the degree of spread (α_{HN}), and the inhomogeneity (β_{HN}) distributions of relaxation oscillators over relaxation times. After reaching (as a result of fitting) a good agreement between the results of calculation by formula (5) and the data of dielectric measurements, it is possible to judge from the values of these parameters about the shape of the distribution function of relaxation oscillators over relaxation times in the material under study (Fig. 5).

The software of modern spectrometers makes it possible to obtain the RT function at the output of the spectrometer with the coefficients τ_{HN}, α_{HN}, and β_{HN}, i.e. the resulting function HN (Fig. 5) is in this sense the result of the experiment.

Interpretation of results

The parameters of the calculated curves shown in Fig. 2, *a* as well as the parameters of the HN function, when fitting the calculated curves to the experimental ones, are selected in such a way as to ensure the best agreement between the results of the calculation of the PS and the measurement results. However, such agreement does not in itself guarantee the complete adequacy of the proposed interpretation of reality. Therefore, to control the correctness of the interpretation of the experimental results, we will use extensive information on the physical properties of vanadium dioxide available in the literature [7,8].

We believe that in our case the values of the PS parameters (the frequency position and shape of the $\varepsilon''(f)$ maximum, the shape and position of the semicircle on the CC-diagram) are due to a specific type of relaxation oscillators, namely, free electrons. The characteristic relaxation time in this case is the Maxwellian relaxation time $\tau_{\mathrm{M}} = \varepsilon\varepsilon_o/\sigma$. At room temperature, for a set of undoped nanocrystalline film grains $\tau_{\mathrm{M1}} = \tau_1 = 2.5 \times 10^{-4}$ s, for a set of grains doped with iron, the Maxwellian time is shorter: $\tau_{\mathrm{M2}} = \tau_2 = 9.9 \times 10^{-6}$ s. Let's explain what has been said.

When all grains of the film are in the semiconductor phase at a temperature of 20°C, i.e. far from the PT temperature ($T_c = 67$°C), the concentration of free electrons in the conduction band is relatively low. Therefore, the electrical conductivity of the film is low, and the Maxwellian relaxation time is large. In this case, $\varepsilon''(f)$ maxima are located at low frequencies (Fig. 2). Nevertheless, the concentration of electrons in the group of Fe-doped grains is higher than in undoped ones; therefore, the maximum *2* corresponding to them is located in the higher-frequency

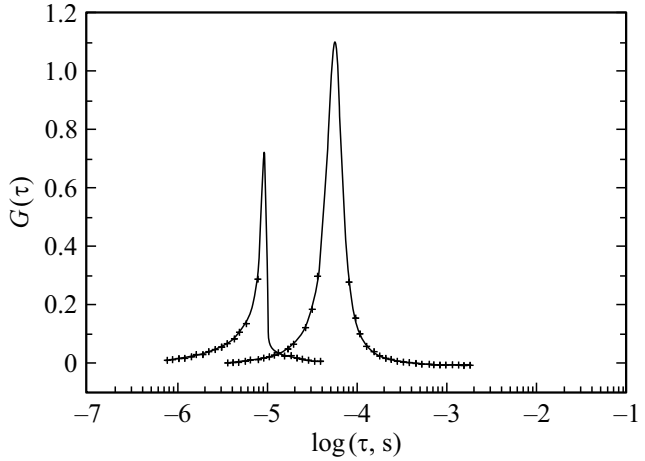

Figure 5. The form of the distribution function HN of relaxation oscillators with respect to relaxation times in accordance with Fig. 2, *b* (ε'') for $T = 20^\circ$ Parameters of the HN function obtained from the approximation of the $\varepsilon''(f)$ curve: $\tau_{HN} = 2.5 \times 10^{-4}$ s, $\alpha_{HN} = 0.06$ and $\beta_{HN} = 0.933$ for maximum *1* and $\tau_{HN} = 9.9 \cdot 10^{-6}$ s, $\alpha_{HN} = 0$ and $\beta_{HN} = 0.706$ for maximum *2*.

region $f_2 = 16400$ Hz (for the totality of undoped grains $f_1 = 840$ Hz).

With an increase in temperature, the concentration of free electrons in the semiconductor phase increases. This increase occurs due to the transition of electrons to the π^*-conduction band. The transition of electrons is accompanied by the destruction of V−V-dimers of the semiconductor phase. The dimers were created by the $d_{x^2-y^2}$-orbitals of V ions forming the lower Hubbard sub-band. This sub-band plays the role of the valence band of the semiconductor. As the specific conductivity σ increases, τ_M decreases, i.e. e. the times $\tau_1 = 1/(2\pi f_1)$ and $\tau_2 = 1/(2\pi f_2)$ are shortened, and the maxima of the $\varepsilon''(f)$ function shift towards higher frequencies.

Note that an increase in temperature by 30°C (from 20°C to 60°C even before the Peierls structural PT shifts the positions of the maxima $\varepsilon''(f)$ towards high frequencies and shortens the relaxation time τ by two orders of magnitude. Such strong changes indicate a rapid thermal increase in the number of relaxation oscillators with short relaxation times. And this is possible only with extremely strong temperature dependence of the concentration of free electrons. This fact indicates that the abrupt Peierls structural PT is preceded by a temperature-stretched electronic Mott PT, which is characteristic of strongly correlated materials, such as VO_2 [9]. With a further increase in temperature (after reaching T_c and performing the structural Peierls PT), the relaxation times τ_1 and τ_2 shorten by one more−two orders.

The experiment shows that the PT temperature in VO_2:Fe films is lower by 5°C than in undoped VO_2 films. The mechanism of the shift by 5°C (down the *T*-hysteresis loop) of the maximum *2* corresponding to nanocrystals doped with iron is as follows.

The electronic configuration of the Fe atom introduced into vanadium dioxide is as follows: (Ar) $[3d^1_{z2}(1)\ 3d^2_{xy}(1)\ 3d^1_{yz}(1)\ 4p^0(3)]\ 3d^1_{xz}(1)\ 3d^1_{x^2-y^2}\ 4s^2(1)4f^0(7)$. Here, the square brackets indicate the orbitals involved in the hybridization required to fix the crystal framework [10], the numbers in brackets indicate the number of orbitals of this type, the superscripts i.e. the number of electrons in them. As we can see, three orbitals are not involved in the framework construction, all of which, in contrast to the V^{4+} ion undoped with VO_2, are occupied by electrons. The principal thing is that the nearest orbital not involved in hybridization and free from electrons is $4f^0$-orbital. The reason for this situation is that the Fe atom differs from the V atom by the population of the *d*-shell: its unfinished *d*-shell has no orbitals free of electrons. So, in Fe, there are 6 electrons on five *d*- levels, which, according to Hund's first rule, occupy all orbitals, and one of them has 2 electrons. And with empty $4f^0$-orbitals, donor-acceptor $4f^0-2p_z^2-\pi$ -bonds with oxygen ions at the corners of the bases of octahedrons. These bonds are included in the formation of the energy position of π- and π^*-zones (similar to $3d^0-2p_z-\pi$-links for V). In this case, the energy π^*-band in VO_2 plays the role of the conduction band [3]. Energy gap between bonding (π) and loosening (π^*) zones for $4f^0-2p_z^2-\pi$-bonds are less than for the $3d^0-2p_z-\pi$-bonds of the V^{4+} ion, according to the Pauling mechanism [11]. The essence of the mechanism is reduced to the statement about the lower energy of those chemical bonds whose orbitals are more strongly shielded by inner electron shells. It follows that doping with Fe ions reduces the band gap VO_2:Fe in proportion to the concentration of ions Fe.

The $3d^1_{x^2-y^2}(1)$ orbital is involved in the formation of Fe−V-dimers similarly to the situation with formation of V−V-dimers in undoped VO_2. However, the binding energy of Fe−V- dimers, according to the same Pauling rule, is also lower than V−V- dimers, due to the shielding of the Fe−V*orbitals*-bonds are additional in relation to the atom V electrons of the *d*-shell (for the Fe atom, the *d*-shell contains 6 electrons instead of 3 for the V atom). The $4s^2(1)$ orbital, being completely saturated, in the first approximation does not participate in the ejection of electrons into the conduction band, similarly, for example, to the fully saturated orbital $2p_z^2$ of an atom oxygen.

Thus, the reduction of T_c in VO_2:Fe is due to the following reasons:

1) the strong decrease in the energy of the π^*-band according to the Pauling dimensional mechanism,

2) some decrease, according to the same mechanism, in the σ-bond energy of Fe−V--dimers from - due to screening of its orbitals by excess electrons *d*- shells of the Fe ion, which facilitates the thermal destruction of dimers.

The experiment shows that in VO_2:Fe the reduction due to T_c from $T_c = 67^\circ$C for undoped VO_2 is half that, for example, in VO_2:W, which corresponds to the proposed

model, as the analysis of the electronic configuration of the tungsten ion.

In conclusion, returning to the calculations of PS and CC-diagrams for different values of the coefficients α and β, we explain the need to introduce coefficients other than 0 and 1 α and β: this is necessary to ensure good agreement between the calculation and experiment and is due to the presence of a size distribution of crystalline grains in the VO_2 : Fe film. As a result, both in doped and undoped grains during fitting, different values of the degree of doping and the associated conductivity σ and, consequently, the Maxwellian relaxation time $\tau = \varepsilon\varepsilon_0/\ sigma$. Therefore, around each relaxation time τ_1 and τ_2, which is characteristic of two types of relaxators (corresponding to the doped and undoped aggregates of VO_2 film grains), there will be note its own distribution of the temporal density of the number of relaxation oscillators. Numerical values α and β characterize, as was indicated, the width and asymmetry of the distribution of the temporal density of relaxation oscillators given by the function HN.

Thus, in this article, one have revealed the features of the electrical response of undoped and Fe-doped vanadium dioxide films synthesized on insulating substrates. The details of the response are manifested in the features of the shape of the PS (steps, maxima, semicircles), as well as the dependence of the frequency position of these features on the sample temperature. The complex picture of the electrical response of the VO_2 : Fe film is due to the difference in the concentration of free electrons in the undoped and Fe-doped nano-crystallites of the VO_2 film, i.e. e. the presence in the total set of nano-crystallites of two types of electrical relaxation oscillators. The found values of the coefficients α and β can be used to estimate the distribution parameters of relaxation times from their values in each individual type of relaxation oscillators, i.e., separately in doped and undoped nano-crystallites of the VO_2 : Fe film.

Funding

The study was supported by the RFBR grant № 20-07-00730.

Conflict of interest

The authors declare that they have no conflict of interest.

References

[1] Fizicheskaya entsiklopediya **1**, 700 (1988) (in RussianI
[2] B.N. Chichkov, C. Momma, S. Nolte, F. Von Alvensleben, A. Tünnermann. Appl. Phys. A, **63** (2), 109 (1996). DOI: 10.1007/BF01567637
[3] A.V. Ilinskiy, O.E. Kvashenkina, E.B. Shadrin. FTP, **46** (4) 439 (2012). [A.V. Ilinskiy, O.E. Kvashenkina, E.B. Shadrin. Semiconductors, **46** (4), 422 (2012). DOI: 10.1134/S1063782612040094].
[4] A.V. Ilinskiy, R.A. Kastro, M.E. Pashkevich, E.B. Shadrin. FTP, **54** (2), 153 (2020). (in Russian). DOI: 10.21883/FTP.2020.02.48910.9267 [A.V. Ilinskiy, R.A. Kastro, M.E. Pashkevich, E.B. Shadrin. Semiconductors, **54** (2), 205 (2020). DOI: 10.1134/S1063782620020116].
[5] A.S. Volkov, G.D. Koposov, R.O. Perfil?ev, A.V. Tyagunin. Opt. i spektr., **124** (2), 206 (2018) (in Russian). DOI: 10.21883/OS.2018.02.45525.200-17 [A.S. Volkov, G.D. Koposov, R.O. Perfiliev, A.V. Tyagunin. Opt. Spectrosc., **124** (2), 202 (2018). DOI: 10.21883/OS.2018.02.45525.200-17].
[6] A.S. Volkov, G.D. Koposov, R.O. Perfilyev. Opt. i spektr., **125** (9), 364 (2018) (in Russian). DOI: 10.21883/OS.2018.09.46552.64-18 [A.S. Volkov, G.D. Koposov, R.O. Perfiliev. Opt. Spectrosc., **125** (9), 379 (2018). DOI:10.1134/S0030400X18090242].
[7] A.V. Ilinskiy,M.E. Pashkevich, E.B. Shadrin. Nauchno-Tekh. Vedomosti SPbGPU. Fiz.-Mat. Nauki, **10**, (3) 9 (2017). (in Russian). DOI: 10.18721/JPM.10301
[8] E.B. Shadrin, A.V. Ilyinsky. FTT, **42** (6), 1092 (2000) [E.B. Shadrin, A.V. Ilinskii. Phys. Solid State, **42** (6), 1126 (2000). DOI: 10.1134/1.1131328].
[9] N.F. Mott. *Metal-Insulator Transitions* (Nauka, M., 1979).
[10] C. Housecroft, E. Constable. *Sovremennyy kurs obshchey khimii* (Mir, M., 2002), 539 p (in Russian). [C.E. Housecroft, E.C. Constable. *Chemistry: An Integrated Approach* (Pearson Education. Limited, Addison. Wesley Longman, 1997), 419 p.].
[11] L. Pauling. *Priroda khimicheskoy svyazi* (Izd. Khim. Lit., M.-L., 1963), 440 p (in Russian). [L. Pauling. *The nature of the chemical bond*, 3rd ed. (Cornell Univ. Publishing. H., 1960), 361 p.].